Hierarchical Assembly of PEG-*b*-Polypeptide Hybrid Block Copolymers on Graphite

Guangzheng Gao, Tao Wang, Junpo He,* Xueqin Chen, and Yuliang Yang

Department of Macromolecular Science, Fudan University, Shanghai 200433, China, and the Key Laboratory of Molecular Engineering of Polymers, Ministry of Education, China

Received October 17, 2006
Revised Manuscript Received January 12, 2007

Introduction

Hybrid block copolymers, or molecular chimeras,[1] composed of synthetic and polypeptide segments exhibit interesting supermolecular structures through hierarchical self-assembly in bulk[1] and in solution.[2] The driving force for the assembly originates from the secondary structure of the peptide. Usually the peptide folds into α-helix and behaves as a rodlike segment. This secondary structure can be combined with coiled conformation of the synthetic segments, such as polystyrene, polybutadiene, poly(ethylene glycol) (PEG), etc., to form rod−coil block copolymers that tend to form hexagonal-in-lamellar morphology in solid state in which the peptide α-helices aligned perpendicular to the lamellar surface.[3] In solution, the rod−coil hybrid copolymer forms not only micelles and vesicles but also unusual aggregates. For instance, amphiphilic block copolymers with polystyrene tail and charged poly(isocyanide) headgroup aggregates into vesicles, bilayer filaments, and superhelices in aqueous solution, depending on pH and counterionic strength.[4] Poly(ferrocenylsilane)-*b*-poly(γ-benzyl-L-glutamate) assembles into a nanoribbon in toluene through 1-dimensional stacking of the block copolymers in a monolayer fashion.[5] On the other hand, the α-helical peptide was also combined with conjugated rigid segments, such as polyfluorene, to yield rod−rod block copolymers that formed a parallel fibrillar textures in the cast film.[6] An interesting feature of the peptide is that it shows helix−coil transition toward the change in pH. This concept was employed independently by Lecommandoux and Klok,[7] as well as Schlaad and co-workers,[8] in the preparation of vesicles from polybutadiene-*b*-polyglutamates with fascinating properties such as pH-responsive shape/size adjustment.

Among hybrid block copolymers with various synthetic segments, those containing PEG blocks received much attention due to their biocompatibilities[9] and potential applications in drug delivery systems.[10,11] Various PEG-*b*-polypeptide copolymers have been synthesized, usually by ring-opening polymerization of amino acid-*N*-carboxyanhydrides (NCA) initiated by the amino end group of PEG.[12] These copolymers form micelles and vesicles in solutions,[13] in resemblance to the conventional amphiphilic block copolymers.[14] However, formation of thermal reversible gels through a nanoribbon mechanism was also reported.[5] In addition, the PEG segment can form inclusion complexes with α-cyclodextrins. The resulting rod−rod peptide-*b*-polypseudorotaxanes were phase separated into bilayers in which columnar hexagonal arrangement of α-helical peptide stacked with channel-type crystallization of the rotaxane segments.[15] Recently, it was found that a graft copolymer, poly(γ-benzyl L-glutamate)-*g*-PEG, also formed micelles in a specific shape of spindle.[16]

We report here the self-assembly of the block copolymers of PEG and peptide on highly oriented pyrolytic graphite (HOPG) observed by atomic force microscopy (AFM). The peptide segment has a structure of poly(γ-stearyl L-glutamate) (PSLG) with *n*-octadecyl side chains. It has been observed by Watanabe and Kunitake and their co-workers using AFM that homopolypeptide with long *n*-alkyl side chains forms 2-dimensional epitaxial arrays on HOPG due to the affinity of alkyl chains toward graphite.[17] We found that the epitaxial adsorption of the *n*-octadecyl side chain also plays an important role in the formation of the aggregates of block copolymers composed of PEG and PSLG segments. In addition, higher order aggregates, such as nanorods and ring-shaped aggregates, were observed beyond the epitaxial adsorption of the peptide segment on the substrate.

Experimental Section

Materials. Dichloromethane (DCM), ethyl acetate, toluene, and dimethylformamide (DMF) were distilled before use. Triphosgene (Acros, 99%), *p*-toluenesulfonyl chloride (Acros, 99%), hydrazine hydrate (Sinopharm Chemical Reagent Co.), 1-octadecanol (Acros, 95%), L-glutamic acid (Acros, 99%), phthalimide potassium salt (Fluka, 99%), and *n*-butyllithium (Acros, 1.3 M in hexane) were used as received. α,ω-Diamino-functionalized PEG (NH_2-PEG-NH_2) and α-methoxy-ω-amino-functionalized poly(ethylene glycol) (MPEG-NH_2) were synthesized from PEG (M_n = 10 000 g/mol, Fluka) and PEG methyl monoether (MPEG, M_n = 5000 g/mol, Fluka) through tosylation[18] and the classic phthalimide−hydrazine procedure.[19] γ-Stearyl L-glutamate (SLG) was synthesized by the reaction between L-glutamic acid and *n*-octadecyl alcohol.[20] γ-Stearyl L-glutamate *N*-carboxyanhydride (SLG-NCA) was prepared according to the literature.[21] White crystals; yield 42%; mp 77−78 °C. ^{1}H NMR (500 MHz, $CDCl_3$): δ 0.88 (t, C*H*$_3$), 1.26 (s, alkyl-C*H*$_2$ chain), 1.62 (m, OCH$_2$C*H*$_2$), 2.20 (m, β-C*H*$_2$), 2.56 (t, γ-C*H*$_2$), 4.10 (t, OC*H*$_2$), 4.39 (t, C*H*), 6.42 (brs, N*H*). ^{13}C NMR (500 MHz, $CDCl_3$): δ 14.06 (*C*H$_3$), 22.65 (*C*H$_2$CH$_3$), 25.84 (OCH$_2$*C*H$_2$), 26.95 (β-*C*H$_2$), 28.48 (γ-*C*H$_2$), 29.21 (OCH$_2$*C*H$_2$), 29.67 (*C*H$_2$), 31.90 (*C*H$_2$CH$_2$CH$_3$), 56.99 (*C*H), 65.52 (O*C*H$_2$), 151.89 (O*C*ONH), 169.46 (O*C*OCH), 172.68 (CH$_2$*C*OO). Anal. Calcd for $C_{24}H_{43}NO_5$: C, 67.73; H, 10.18; N, 3.29. Found: C, 67.56; H, 10.26; N, 3.35.

Syntheses. The di- and triblock PEG and PSLG copolymer samples were prepared by ring-opening polymerization of SLG-NCA initiated by MPEG-NH_2 and NH_2-PEG-NH_2.[22] Here is an example for the synthesis of diblock copolymer, PEG-*b*-PSLG. MPEG-NH_2 (M_n = 5000 g/mol, 0.12 g, 0.024 mmol) was dissolved in DCM (4 mL), and then SLG-NCA (0.41 g, 0.96 mmol) in 4 mL of DCM was added into the solution. The reaction mixture was stirred at 30 °C for 72 h. The product was precipitated twice from ethyl ether (40 mL) and dried. White powder, 71%. $M_{n,GPC}$ = 8900 g/mol; M_w/M_n = 1.20.

The synthesis and characterization of di- and triblock copolymers are summarized in Table 1.

Measurements. FT-IR spectra were measured on a Nicolet Magna-550 FT-IR instrument using a KBr pellet of fixed thickness. Circular dichroism (CD) experiments were carried on a Jasco J-715 spectropolarimeter by using a 0.1 cm quartz cell at room temperature in THF. ^{1}H NMR spectra were recorded on Bruker (500 MHz) NMR instrument using $CDCl_3$ as the solvents and tetramethylsilane (TMS) as the reference. The number- and weight-average molecular weights (M_n and M_w) of polymers were determined by gel permeation chromatography (GPC) through three Waters Styragel

* Corresponding author: Fax +86-21-6564-0293; e-mail jphe@fudan.edu.cn.

10.1021/ma062386p CCC: $37.00
Published on Web 02/28/2007

Table 1. Characterization of Hybrid Block Copolymers

sample	M_n[a]	M_w/M_n[a]	n[b]	$[\theta]_{222}$[c] (deg cm^2/dmol)	amide I (cm^{-1})[d]	amide II (cm^{-1})[d]
PEG_{113}-*b*-$PSLG_{41}$	8900	1.20	41	−35813	1656	1548
$PSLG_{66}$-*b*-PEG_{227}-*b*-$PSLG_{66}$	31700	1.45	66	−43541	1655	1549

[a] Determined by GPC calibrated by polystyrene standards; eluent: THF. [b] Polymerization degree of PSLG block of copolymers (determined by ^{1}H NMR). [c] Determined by CD in THF. [d] Determined by FTIR, KBr pellets.

Scheme 1

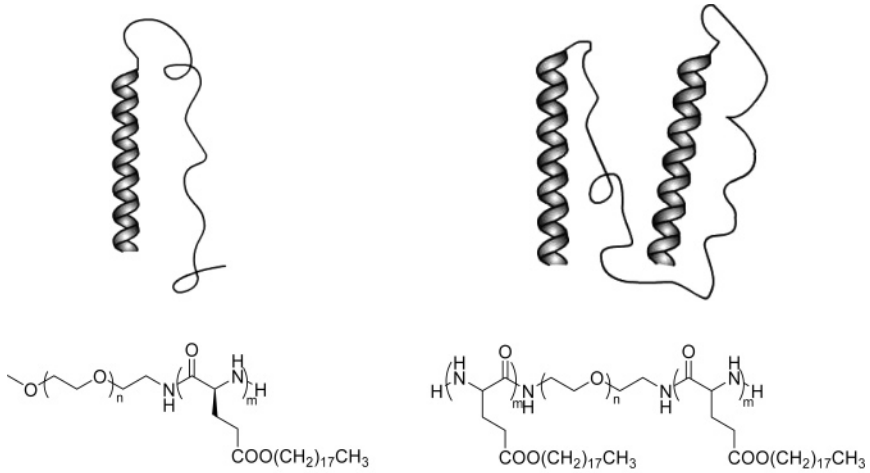

PEG_{113}-*b*-$PSLG_{41}$ **$PSLG_{66}$-*b*-PEG_{227}-*b*-$PSLG_{66}$**

columns (pore size: 10^2, 10^3, and 10^4 Å in series) in a Waters 2010 system, using THF as eluent at a flow rate of 1 mL/min at 40 °C. The columns were calibrated with narrow polystyrene standards (MW range 2.2×10^3−1.94×10^5 g/mol). AFM observation was performed on an instrument of NanoScope IV (Digital Instruments, Santa Barbara, CA) operated at tapping mode, using silicon tips of Model TESP (Digital Instruments) with radius of curvature of the tip less than 10 nm. Three force levels, namely hard ($A_{sp}/A_0 = 0.40$−0.60), moderate ($A_{sp}/A_0 = 0.60$−0.80), and light ($A_{sp}/A_0 = 0.80$−0.99) tapping force, based on set-point ratios were employed.[23] Polymer solution was spin-coated (2000 rpm) or drop-cast (3−5 μL) on the surface of freshly cleaved HOPG (Digital Instruments). X-ray photoelectron spectroscopy (XPS) was performed on a RBD upgraded PHI-5000C ESCA system (Perkin-Elmer) with Mg Kα radiation ($h\nu = 1253.6$ eV). In general, the X-ray anode was run at 250 W, and the high voltage was kept at 14.0 kV with a detection angle at 54°. The base pressure of the analyzer chamber was about 5×10^{-8} Pa. The whole spectra (0−1100 eV) and the narrow spectra of all the elements with much high resolution were both recorded by using RBD 147 interface (RBD Enterprises) through the AugerScan 3.21 software. Binding energies were calibrated by using the contaminant carbon (C 1s = 284.6 eV). The data analysis was carried out by using the RBD AugerScan 3.21 software provided by RBD Enterprises. The static contact angle was measured on OCA15 (Dataphysics, Germany) equipped with a digital camera. Droplets of distilled water (about 3 μL) were dropped on sample surface, and at least six independent measurements were taken to determine average values.

Results and Discussion

The di- and triblock copolymers, PEG_{113}-*b*-$PSLG_{41}$ and $PSLG_{66}$-*b*-PEG_{227}-*b*-$PSLG_{66}$, are highly soluble in organic solvents such as THF, CH_2Cl_2, and $CHCl_3$ at room temperature. IR spectra of the block copolymers show peaks at ∼1655 cm^{-1} (amide I) and ∼1549 cm^{-1} (amide II) (see Table 1 and Supporting Information), indicative of a perfect α-helical conformation of the peptide block.[24] CD spectra show two negative peaks at 208 and 222 nm which are ascribed to the right-handed α-helix structure (Supporting Information). The helix contents of PEG_{113}-*b*-$PSLG_{41}$ and $PSLG_{66}$-*b*-PEG_{227}-*b*-$PSLG_{66}$ were calculated to be 83 and 100% based on the intensities at 222 nm, respectively.[25] Thus, the diblock and triblock copolymers adopt rod−coil conformations as shown schematically in Scheme 1. The self-assembly of the block copolymers were then observed by AFM using HOPG as the substrate.

First, the block copolymer, PEG_{113}-*b*-$PSLG_{41}$, was spin-coated onto HOPG from a dilute solution in chloroform (2×10^{-6} mol/L based on amino acid unit). AFM images in Figure 1 show islandlike domains scattered randomly on the surface of the graphite (dark background). In the height images (Figure 1a,c), the islands are quite irregular in shape, with some fine structures underneath. The fine structures are clearly visible in phase images (Figure 1b,d) as rods aligned in parallel direction in each domain. The running direction, marked by arrows in Figure 1d, displays a cross angle of 60° between rods in different islands. The striped pattern of the domain is assigned to the aggregate of α-helices of peptide blocks. Previously, the aggregation of homopolypeptide with long alkyl chains was thoroughly investigated by Kunitake and Watanabe and co-workers.[17] They found that poly(γ-*n*-alkyl L-glutamates) formed two-dimensional arrays through epitaxial adsorption of alkyl chains on HOPG. The alkyl chains accommodated extended, all-trans conformation at both sides of helical peptide and aligned perpendicularly to the helical peptide.[17] The fine structure observed in the present work correlates very well with the model proposed by Watanabe and co-workers[17] for homopolypeptide and is therefore ascribed to the epitaxial arrangement of the peptide segment, as shown in Figure 1e. The interval distances between the parallel rods are about 6.10 ± 0.19 nm, which is roughly double of the stretched length of stearyl side chains and agrees well with the result in the literature (Figure 4 in ref 17). The cross-angle of 60° between different domains is attributed to the ⟨1210⟩ direction of HOPG according to ref 17.

Thus, the polypeptide block in PEG_{113}-*b*-$PSLG_{41}$, resembling homopolypeptide, forms epitaxial aggregates due to affinity of the stearyl side chain toward the surface of the graphite (see Figure 1e). The striped aggregates are surrounded or covered

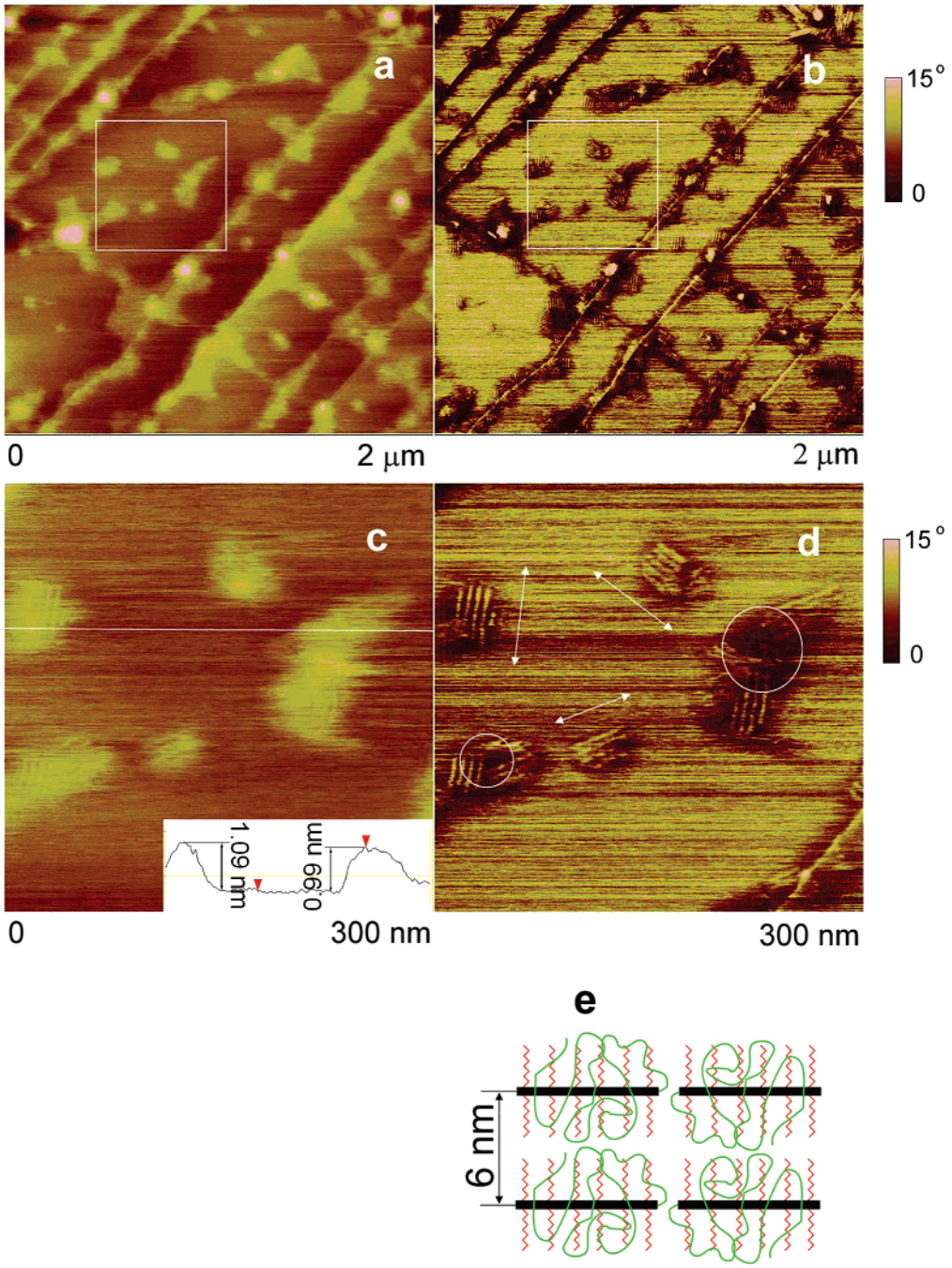

Figure 1. AFM images of spin-coated sample, PEG_{113}-*b*-$PSLG_{41}$ (2×10^{-6} mol/L in $CHCl_3$), on HOPG. (a) Height image. (b) Phase image. (c) High-resolution image of selected region in (a) (indicated by the white frame). (d) High-resolution image of selected region in (b) (indicated by the white frame). (e) Proposed model for the self-assembly of PEG_{113}-*b*-$PSLG_{41}$ on HOPG, in which the black rods, zigzag lines, and green coils represent peptide helices, alkyl chains in all-trans conformation, and PEG coils, respectively. The green coils stay above or surrounding the helices and the stretched alkyl chains.

by a cloud of PEG coil, as evidenced by the height images in Figure 1a,c. The cross section indicates that the average corrugations of the islands are 0.86 ± 0.22 nm, which is much higher than that expected for pure poly(γ-stearyl L-glutamate), and display hill-like profiles in contrast to the constant values measured by Kunitake[17] for homopolypeptide. The remarkable variation in height values reflects the irregular shape of PEG cloud and is also a consequence of the overlapping of PEG clouds at the border of different domains, as indicated by the circles in Figure 1d.

It is noteworthy that the lengths of the rods, ranging from 20 to 60 nm, are much larger than the length of a single α-helix formed by peptide block, which is estimated as 6.15 nm according to the degree of polymerization (DP = 41, by NMR).[6,15] The same phenomenon was also observed in homopolypeptide and was ascribed to "head to head" or "head to tail" intermolecular arrangement.[17] In the present work, it is expected that the presence of PEG segment would hamper arrangement in such a mode. Nevertheless, each strip shown by AFM consists of 3−9 PSLG blocks according to the length. It is deduced that the propensity of epitaxial assembly of PSLG segment, with the aid of intermolecular van der Waals interactions of alkyl chains, is so strong that PEG segments are excluded from the striped pattern, forming a surrounding cloud to the domain.

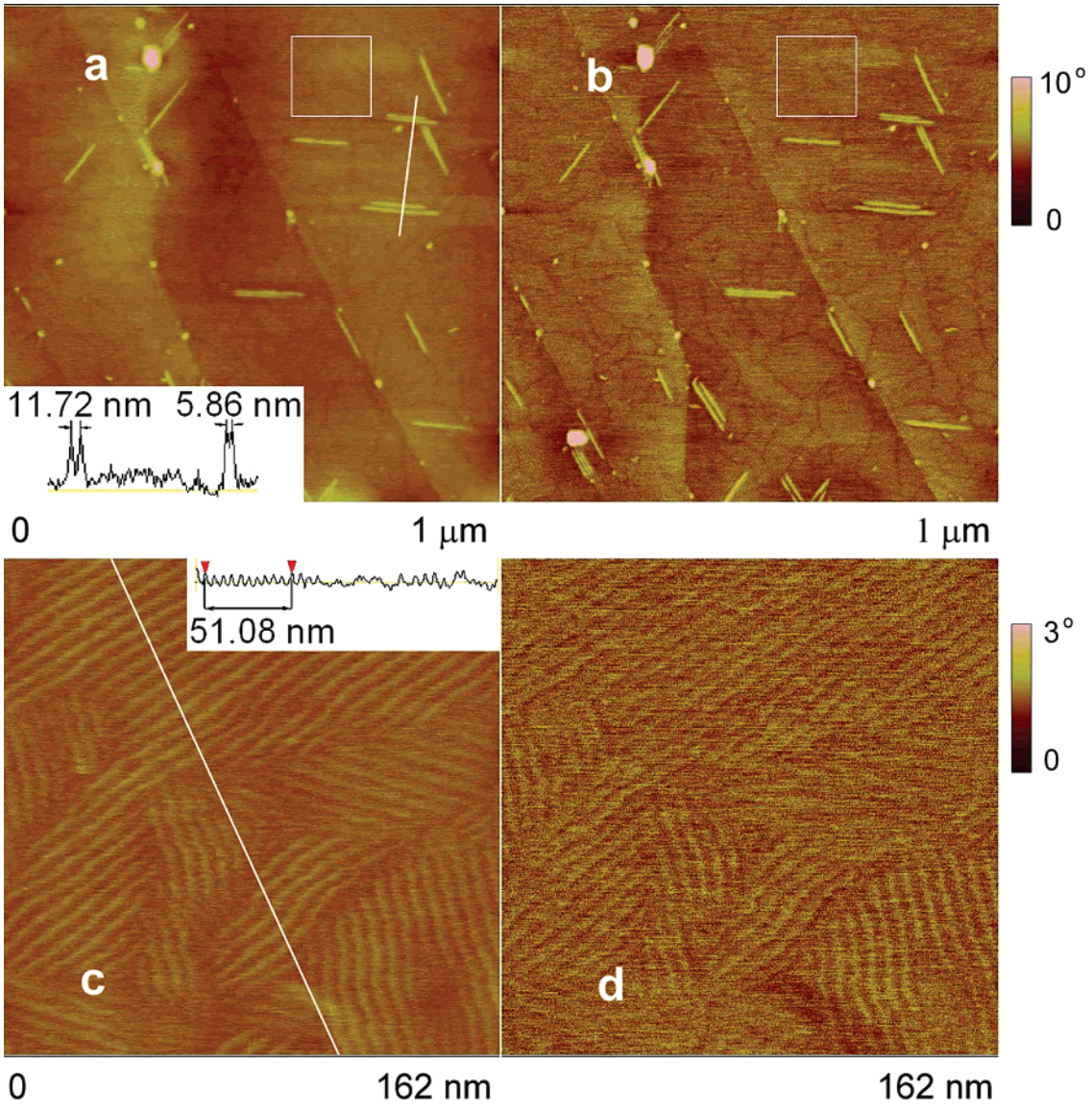

Figure 2. AFM images of PEG_{113}-*b*-$PSLG_{41}$ (2×10^{-6} mol/L in $CHCl_3$) on HOPG by drop-casting. (a) Height image, (b) Phase image, (c) High-resolution image of selected region in (a) (indicated by the white frame). (d) High-resolution image of selected region in (b) (indicated by the white frame).

In the second experiment, the same solution of the block copolymers (2×10^{-6} mol/L in chloroform) was drop-cast, instead of spin-coated, onto HOPG. Figure 2 shows the morphologies observed by AFM operated at moderate tapping force for PEG_{113}-*b*-$PSLG_{41}$. It is interesting to find two kinds of aggregates exist simultaneously in the sample. In the wide view (Figure 2a,b), larger nanorods of ~100 nm in length and 1.13 ± 0.18 nm in height scattered on a substrate layer. A close analysis by fine scanning (Figure 2c,d) reveals that the substrate layer is a densely packed monolayer formed by epitaxial assembly of the peptide segments. The monolayer is composed of different domains with different sizes and irregular shapes. Similar to that in spin-coated sample, within each domain the helices adopt parallel alignment, and a cross-angle of 60° is observed between different domains. The distance between these helices within each domain is 5.21 ± 0.20 nm (inset in Figure 2c), which is slightly less than that of the spin-coated sample and attributable to partly interdigitated arrangement between alkyl side chains of PSLG segment.[17] Above the monolayer, there should exist a layer of excluded PEG coils that covers the ordered pattern. Indeed, it was found that the striped pattern of the monolayer could not be detected using light tapping force, possibly due to the mask of the PEG layer.

The nanorods above the monolayer run in same directions as the underlying striped pattern and show a rotation angle of 60° as well. Most of the rods exist in a single mode, but some appear in two kinds of pairs, the contact pair with an interval of about 5.86 nm and the loose pair 11.72 nm (Figure 2a). Since the interval of the contact pair is very close to that of the epitaxial layer (Figure 1e), we propose that the nanorods scattered on the substrate was formed through the second layer epitaxial adsorption of peptide segments guided by the "rail effect"[26,27] of the substrate. By this model, the much larger width of the nanorods (21.87 ± 2.34 nm) is ascribed to the "tip broadening effect" of the AFM probe. The fact that the larger nanorods tend to exist in a single mode is in sharp contrast to the assembly of peptide helices directly on HOPG, in which single rods has never been observed even with very dilute solution (vide infra). This implies that the lateral assembly of the larger nanorods is interrupted by PEG segments of themselves and of the lower layer.

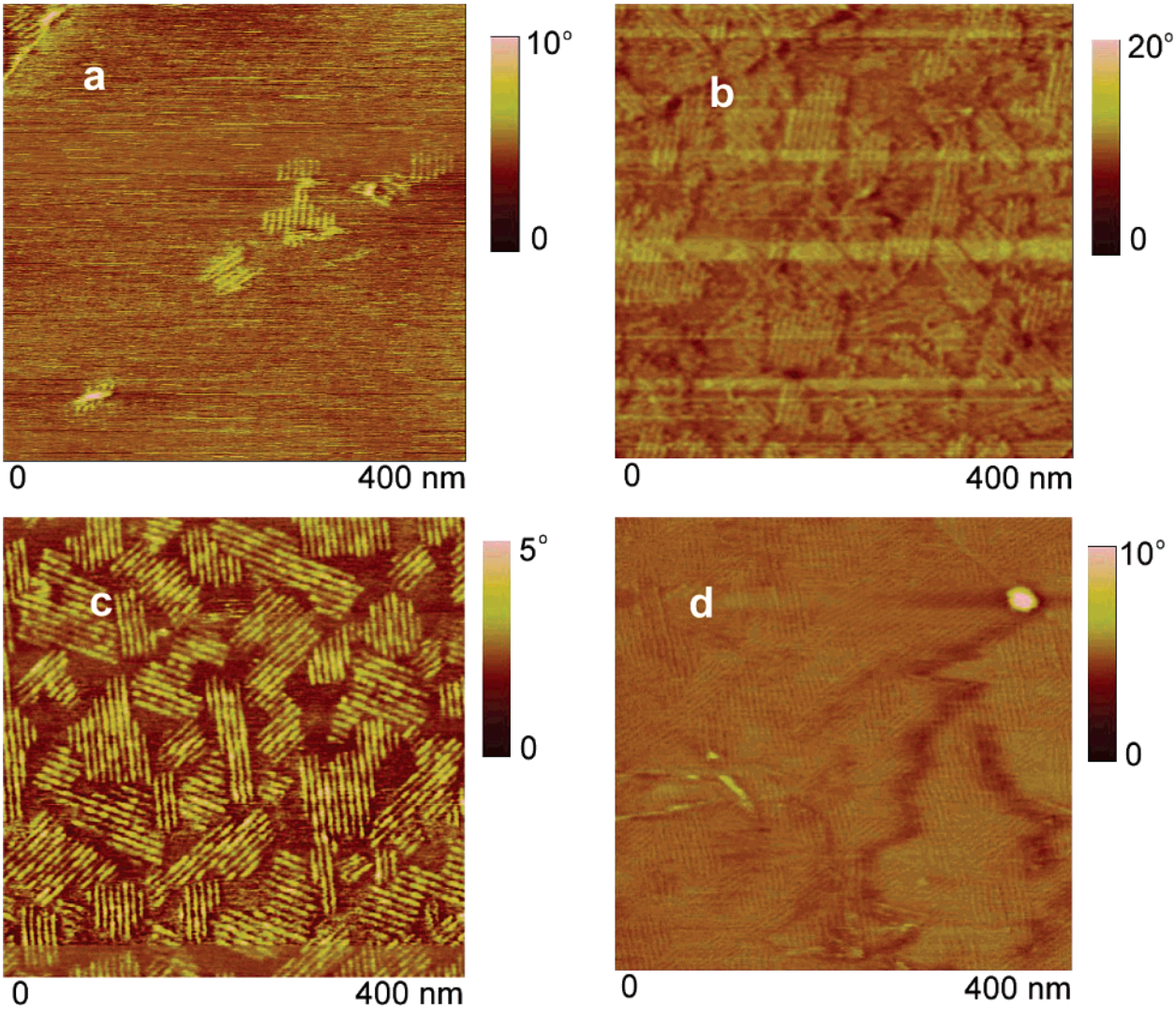

Figure 3. AMF phase images of samples by drop-casting from chloroform solutions of PEG_{113}-*b*-$PSLG_{41}$ with the concentration of (a) 1.0×10^{-6}, (b) 1.3×10^{-6}, (c) 1.5×10^{-6}, and (d) 2.0×10^{-6} mol/L.

We varied the solution concentration of diblock copolymer to investigate its influence on the morphology in drop-casting method. Figure 3 shows that the very dilute solution results in scattered domains on the substrate, similar to that in spin-coating. With the increase in concentration, the domains become larger in size and in number until the full coverage of the area for the applied concentration of 2.0×10^{-6} mol/L. This demonstrates that the key factor determining the morphology is the quantity of polymers deposited on HOPG, not the preparatory method, i.e., spin-coating and drop-casting. The reason for the scattered domains virtually observed in the former is that part of the polymers were spun off during the preparation process.

The monolayer prepared by drop-casting from the solution of 2.0×10^{-6} mol/L was investigated by XPS, contact angle measurement, and AFM probe scratching (Supporting Information). In the XP wide scan spectrum, C 1s and N 1s were observed at 284.6 and 399.7 eV, respectively. The core level spectrum of C 1s shows binding energy of 284.6, 286.1, 287.5, and 288.5 eV for C−C, C−O/C−N, C(═O)N, and C(═O)O moieties, respectively. The contact angles of the monolayers of both diblock and triblock copolymers are 80°, in contrast to that of HOPG, 90°, and of a homopolypeptide, PSLG, 92°, respectively, indicating an increased hydrophilic property of the block copolymers. Nevertheless, the monolayer has a very low thickness, ∼0.77 nm, as measured using a probe scratch technique[28] in which the film was scratched to the plane of HOPG (Supporting Information).

In the third experiment, relatively concentrated solutions (4.0×10^{-6} mol/L based on amino acid units) of the di- and triblock copolymers, PEG_{113}-*b*-$PSLG_{41}$ and $PSLG_{66}$-*b*-PEG_{227}-*b*-$PSLG_{66}$, were drop cast onto HOPG. Figure 4 shows morphologies observed by AFM using light and moderate tapping force. Under the former, circular aggregates formed by PEG_{113}-*b*-$PSLG_{41}$ were observed, with diameters 105 ± 26 nm (Figure 4a). Under the latter, the circular aggregates were found to have a hollow (or soft) center, with outer diameters 130 ± 19 nm and inner diameters 46 ± 12 nm (Figure 4b). Meanwhile, the height of the circular aggregates is 1.54 ± 0.44 nm under light tapping force and is reduced to 0.65 ± 0.22 nm with the moderate tapping force. This means that the aggregates are flat circular in shape, of which the height is close to the thickness of the monolayer of the block copolymers. Since the outer diameter of the sphere is more than 2-fold of the stretched length of the copolymers (47 nm),[15] we propose a ring-shaped model (Figure 4c), in which the ring is formed by a 2D bilayer of the block copolymers. Similar aggregates were also observed by casting $PSLG_{66}$-*b*-PEG_{227}-*b*-$PSLG_{66}$ on HOPG (Figure 4d−f).

Keeping in mind that all of the solution concentrations in this work are far below the cmc of the hybrid block copolymers,

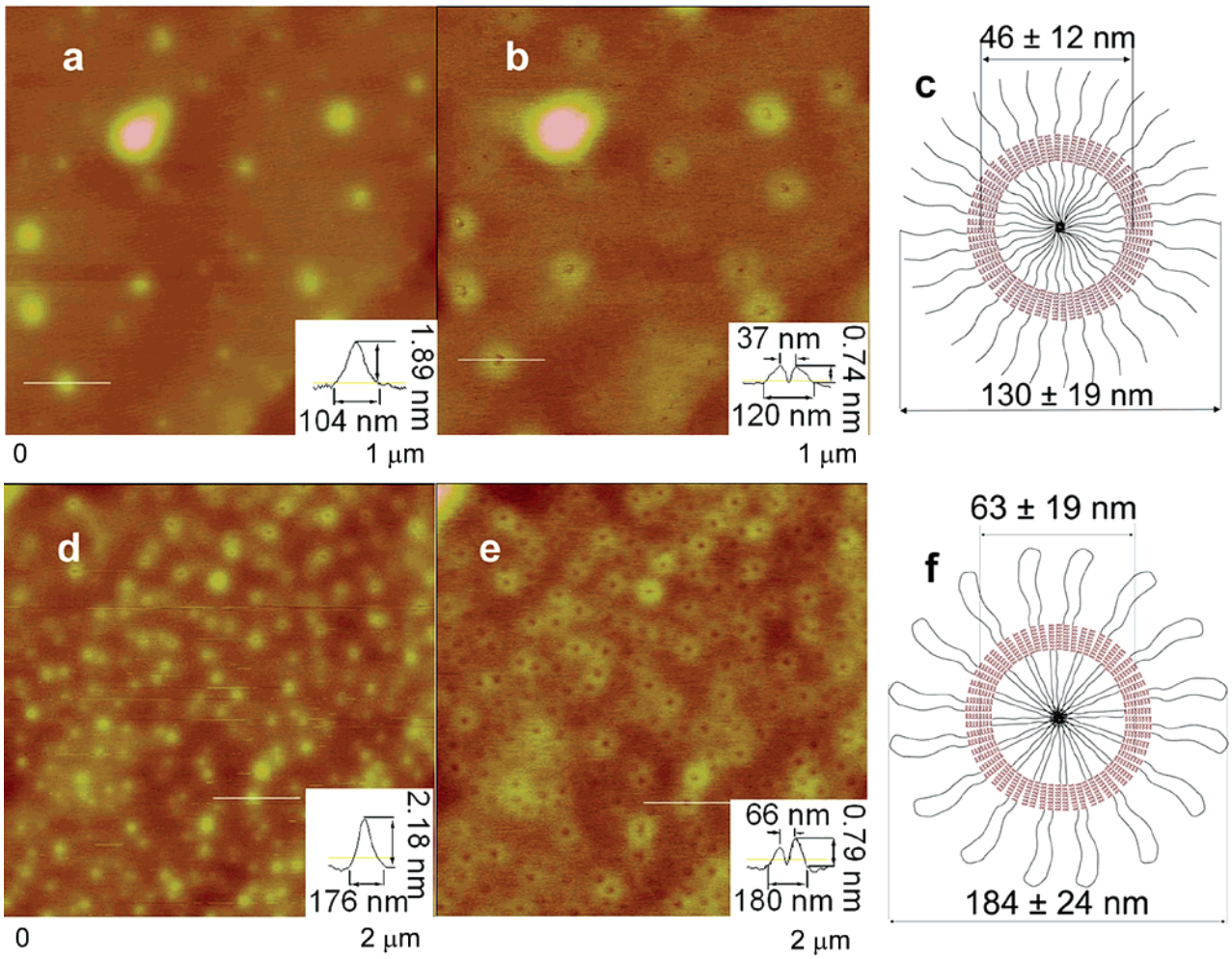

Figure 4. AFM height images of ring-shaped aggregates of PEG_{113}-*b*-$PSLG_{41}$ (a, b) and $PSLG_{66}$-*b*-PEG_{227}-*b*-$PSLG_{66}$ (d, e) (both 4×10^{-6} mol/L in $CHCl_3$) on HOPG using light (a, d) and moderate (b, e) tapping force, respectively, with the proposed models for the aggregates of PEG_{113}-*b*-$PSLG_{41}$ (c) and $PSLG_{66}$-*b*-PEG_{227}-*b*-$PSLG_{66}$ (f) on HOPG.

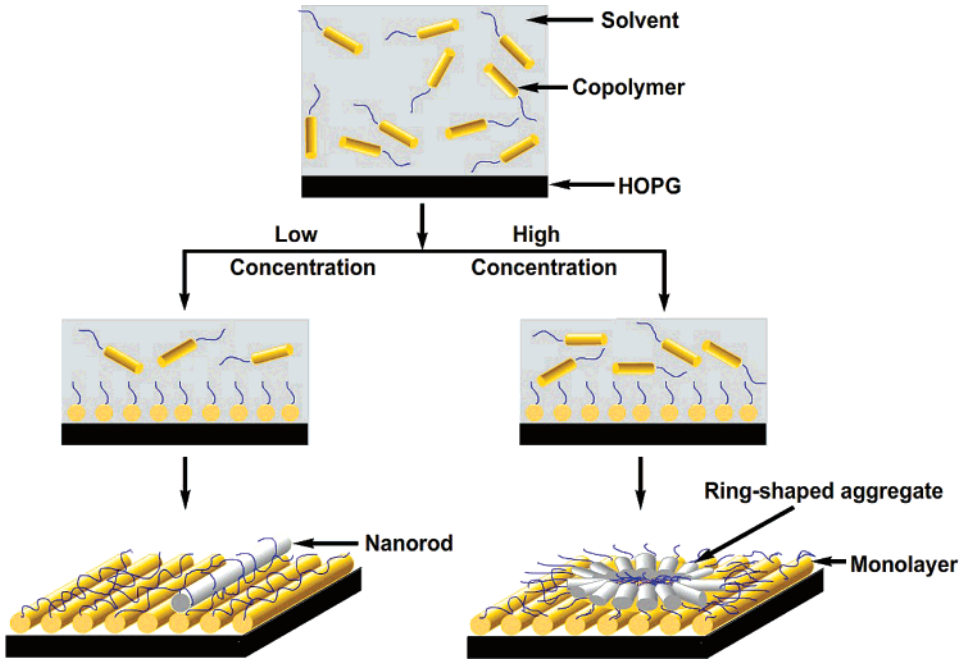

Figure 5. Schematic drawing of the mechanism of nanorod and ring-shaped morphologies. The aggregates and the rods of the monolayer are different in color only for guiding the eyes.

we propose a two-step process for the formation of the observed morphologies. As interpreted in Figure 5, expitaxial adsorption immediately takes place after the casting of the block copolymer solution, while the solvent is evaporating. In this first step the

adsorption is fast and dominant. With very dilute solution, the amount of block copolymers does not suffice the covering of the whole area of HOPG, leaving scattered domains in which striped pattern of peptide helices is surrounded and covered by clouds of PEG segment. With medium concentration, epitaxial adsorption of peptide helices leads to the formation of a monolayer covered by PEG segments. However, there is small quantity of remaining block copolymers after the adsorption. These surplus copolymers undergoes second layer epitaxial adsorption guided by the "rail effect" of the first layer, resulting in nanorod scattered on the surface of the monolayer. With larger concentration, the amount of surplus copolymers is larger and exceeds critical micellization concentration (cmc) during the evaporation of the solvent. The block copolymers used in the present work, like many amphiphilic block copolymers,[29] can self-assemble into micelle or vesicles in solution. At this time, however, the larger part of the solvent has evaporated. The locus for the further assembly is a monolayer with PEG brushes, covered by a very thin layer of the solvent. This very specific space-limiting environment leads to the formation of the ring-shaped aggregates, which are composed of outer and inner PEG segments and middle peptide segments. The morphologies and the style of aggregation in this work are similar to those planar structures in Langmuir−Blodgett film formed by block copolymers at air−water interface.[30−33]

Conclusion

Block copolymers containing peptide segment with alkyl side chains undergo hierarchical self-assembly on HOPG through epitaxial adsorption of the peptide segment. The morphologies depend on the quantity of block copolymers deposited on the substrate. With increasing concentrations, block copolymers self-assemble into islandlike aggregates, monolayer, monolayer with larger nanorods, and monolayer with ring-shaped aggregates. These diverse morphologies are results of hierarchical assembly of block copolymers, induced from peptide's folding into α-helix, epitaxial adsorption onto HOPG, rod−coil contrast and amphiphlicity, and the space limitation of the preparatory location.

Acknowledgment. This work was subsidized by the National Basic Research Program of China (2005CB623800). J.H. and Y.Y. thank NSFC program "Excellence in Research Groups" and "Excellence in Doctorial Dissertation" (200324).

Supporting Information Available: IR and CD spectra of PEG_{113}-*b*-$PSLG_{41}$ and $PSLG_{66}$-*b*-PEG_{227}-*b*-$PSLG_{66}$, AFM images of PSLG on HOPG, XP spectra of a sample prepared by drop-casting from chloroform solution of PEG_{113}-*b*-$PSLG_{41}$, water contact angle on various surfaces, and AFM images of a scratched sample prepared by drop-casting from the solution of PEG_{113}-*b*-$PSLG_{41}$. This material is available free of charge via the Internet at http://pubs.acs.org.

References and Notes

(1) Schlaad, H. Antonietti, M. *Eur. Phys. J. E* **2003**, *10*, 17−23.
(2) Schlaad, H. *Adv. Polym. Sci.* **2006**, *202*, 53−73.
(3) Douy, A.; Gallot, B. *Polymer* **1982**, *23*, 1039−1044.
(4) Cornelissen, J. J. L. M.; Fischer, M.; Sommerdijk, N. A. J. M.; Nolte, R. J. M. *Science* **1998**, *280*, 1427−1430.
(5) Kim, K. T.; Park, C.; Vandermeulen, G. W. M.; Rider, D. A.; Kim, C.; Winnik, M. A.; Manners, I. *Angew. Chem., Int. Ed.* **2005**, *44*, 7964−7968.
(6) Kong, X.; Jenekhe, S. A. *Macromolecules* **2004**, *37*, 8180−8183.
(7) Chécot, F.; Lecommandoux, S.; Gnanou, Y.; Klok, H.-A. *Angew. Chem., Int. Ed.* **2002**, *41*, 1340−1343.
(8) Kukula, H.; Schlaad, H.; Antonietti, M.; Förster, S. *J. Am. Chem. Soc.* **2002**, *124*, 1658−1663.
(9) Vandermeulen, G. W. M.; Tziatzios, C.; Duncan, R.; Klok, H.-A. *Macromolecules* **2005**, *38*, 761−769.
(10) Osada, K.; Kataoka, K. *Adv. Polym. Sci.* **2006**, *22*, 113−153.
(11) Thünemann, A. F.; Beyermann, J.; Kukula, H. *Macromolecules* **2000**, *33*, 5906−5911.
(12) (a) Li, J.; Kao, W. J. *Biomacromolecules* **2003**, *4*, 1055−1067. (b) Deming, T. J. *Adv. Polym. Sci.* **2006**, *22*, 1−18.
(13) Kimura, S.; Kim, D.-H.; Sugiyama, J.; Imanishi, Y. *Langmuir* **1999**, *15*, 4461−4463.
(14) Gohy, J.-F. *Adv. Polym. Sci.* **2005**, *190*, 65−136.
(15) Lee, H.-F.; Sheu, H. S.; Jeng, U-S.; Huang, C.-F.; Chang, F.-C. *Macromolecules* **2005**, *38*, 6551−6558.
(16) Tang, D.; Lin, J.; Lin, S. Zhang, S.; Chen, T.; Tian, X. *Macromol. Rapid Commun.* **2004**, *25*, 1241−1246.
(17) Imase, T.; Ohira, A.; Okoshi, K.; Sano, N.; Kawauchi, S.; Watanabe, J.; Kunitake, M. *Macromolecules* **2003**, *36*, 1865−1869.
(18) Vos, R. J. D.; Goethals, E. J. *Makromol. Chem., Rapid Commun.* **1985**, *53*, 53−56.
(19) Pillai, V. N. R.; Mutter, M.; Bayer, E.; Gatfield, I. *J. Org. Chem.* **1980**, *45*, 5364−5370.
(20) Wasserman, D.; Garber, J. D.; Meigs, F. M. U.S. Patent 3285953, 1966.
(21) Poche, D. S.; Moore, M. J.; Bowles, J. L. *Synth. Commun.* **1999**, *29*, 843−854.
(22) Kim, G.; Kim, J.-Y.; Sohn, D. *Macromol. Res.* **2002**, *10*, 49−52.
(23) (a) Raghavan, D.; Gu, X.; Nguyen, T.; Vanlandingham, M.; Karim, A. *Macromolecules* **2000**, *33*, 2573−2583. (b) Wang, Y.; Song, R.; Li, Y.; Shen, J. *Surf. Sci.* **2003**, *530*, 136−148.
(24) (a) Blout, E. R.; Asadourian, A. *J. Am. Chem. Soc.* **1956**, *78*, 955−961. (b) Miyazawa, T.; Blout, E. R. *J. Am. Chem. Soc.* **1961**, *83*, 712−719. (c) Jeon, S.; Choo, J.; Sohn, D.; Lee, S. N. *Polymer* **2001**, *42*, 9915−9924.
(25) Myer, Y. P. *Macromolecules* **1969**, *2*, 624−428.
(26) Severin, N.; Barner, J.; Kalachev, A. A.; Rabe, J. P. *Nano Lett.* **2004**, *4*, 577−579.
(27) Sakurai, S.-i.; Okoshi, K.; Kumaki, J.; Yashima, E. *Angew. Chem., Int. Ed.* **2006**, *45*, 1245−1248.
(28) Percec, V.; Rudick, J. G.; Wagner, M.; Obata, M.; Mitchell, C. M.; Cho, W.-D.; Magonov, S. N. *Macromolecules* **2006**, *39*, 7342−7351.
(29) Terreau, O.; Soo, P. L.; Duxin, N.; Eisenberg, A. Self-assembly of block copolymer aggregates in solution- Introdution. In *Macromolecular Self-Assembly*; Jiang, M., Ed.; Science Press: Beijing, 2006.
(30) Zhu, J.; Lennox, R. B.; Eisenberg, A. *J. Phys. Chem.* **1992**, *96*, 4727−4730.
(31) Li, S.; Hanley, S.; Khan, I.; Varshney, S. K.; Eisenberg, A.; Lennox, R. B. *Langmuir* **1993**, *9*, 2243−2246.
(32) Cox, J. K.; Yu, K.; Constantine, B.; Eisenberg, A.; Lennox, R. B. *Langmuir* **1999**, *15*, 7714−7718.
(33) Zhang, J.; Cao, H.; Wan, X.; Zhou, Q. *Langmuir* **2006**, *22*, 6587−6592.

MA062386P